Nonequilibrium velocity distributions in liquids: Systems under shear

T. Croteau and D. Ronis
Department of Chemistry, McGill University, 801 Sherbrooke Ouest, Montréal, Québec, Canada H3A 2K6
(Received 16 August 2002; published 10 December 2002)

A Green-Kubo expression for the nonequilibrium correction to the velocity distribution function is studied in a molecular dynamics simulation for systems interacting through a 6-12 potential and undergoing linear shear. As a function of velocity, the first correction to the distribution function has a form similar to what would be obtained from the Boltzmann-Enskog equation, although the amplitude is qualitatively different, except at infinite dilution. The difference comes from elastic effects seen in the short-time behavior of the underlying time correlation functions.

DOI: 10.1103/PhysRevE.66.066109 PACS number(s): 05.10.−a, 05.60.−k, 05.20.Dd, 47.70.Nd

I. INTRODUCTION

The study of distributions and correlation functions in nonequilibrium systems is a central problem in statistical mechanics. In dilute gases, the Boltzmann equation [1,2] or its generalizations [3] are the usual starting points, while in dense systems, several approaches have been used, some phenomenological, some based on kinetic theory, and others on linear response theory [4]. Much of this work focused on the configurational distribution function, which exhibits long-ranged correlations in simple nonequilibrium steady states [5–7], thereby making them more amenable to measurement. Nonetheless, there are nonequilibrium corrections to the velocity distribution, and while hard to measure directly, they are easy to probe indirectly through their contributions to the nonequilibrium stress, heat current, etc. In this work, we will examine the corrections to the velocity distribution function in systems linearly displaced from equilibrium, and, in particular, will apply the theory to fluid systems subjected to a linear shear gradient.

The approach we follow is based on Kubo's linear response theory [8] and was used to consider correlations in simple nonequilibrium fluid systems [5–7]. This theory is summarized in Sec. II with the particular goal of the linear correction to the velocity distribution function in mind. We end up with a modified Green-Kubo expression for the correction, and this is calculated in a molecular dynamics simulation of particles interacting through a 6-12 potential. The results of the simulation are presented and discussed in Sec. III. Two of these results are noteworthy. First, the underlying Green-Kubo time correlation functions all show a short-time increase, which is analyzed in detail in the Appendix. Second, the functional form of the correction to the velocity correlation function is well described by a one Sonine polynomial expansion, just as is found in the Boltzmann and Boltzmann-Enskog equations, *even at liquid densities*. The coefficient of this expansion is qualitatively different from that found in the Boltzmann and Boltzmann-Enskog approaches, the difference being related to the short-time effects. Finally, Sec. IV contains some concluding remarks.

II. THEORY

A. Linear response

In this section, we briefly summarize the derivation of a linear constitutive relation for an arbitrary mechanical quantity B, using Kubo's linear response theory (cf. Ref. [8]) presented in Ref. [5]. The fundamental microscopic equation governing the behavior of the distribution function or density matrix in classical or quantum nonequilibrium statistical mechanics is the Liouville equation, i.e.,

$$\frac{\partial f(t)}{\partial t} = -iL(t)f(t), \tag{2.1}$$

where $f(t)$ is the distribution function or density matrix, the Liouville operator is defined as

$$iL(t)A \equiv \begin{cases} \{A,H(t)\}, & \text{classical,} \\ \dfrac{i}{\hbar}[A,H(t)], & \text{quantum,} \end{cases} \tag{2.2}$$

and where $\{\ldots,\ldots\}$ and $[\ldots,\ldots]$ denote Poisson brackets and a commutator, respectively. Following Kubo [8], we write

$$H(t) \equiv H_0 + H_1(t) \tag{2.3}$$

and

$$L(t) \equiv L_0 + L_1(t), \tag{2.4}$$

where H_0 governs the behavior of our system at equilibrium while $H_1(t)$ is responsible for taking the system out of equilibrium, and is written as

$$H_1(t) \equiv -\mathsf{A}*\mathsf{F}(t) \equiv -\sum_\alpha \int d\boldsymbol{r} A_\alpha(\boldsymbol{r}) F_\alpha(\boldsymbol{r},t), \tag{2.5}$$

where $F_\alpha(\boldsymbol{r},t)$ is an external field, and where $A_\alpha(\boldsymbol{r})$ is a mechanical variable or operator. (We use sans serif type to denote a column vector of variables.)

If Eq. (2.1) is solved perturbatively to first order in the external fields and the result used to compute the average of a mechanical variable B, it follows that

$$\hat{b}(t) \equiv \langle B(t)\rangle_{NE} - \langle B\rangle \sim -\beta \int_{-\infty}^{t} ds \langle \dot{B}_{Kubo}(t-s)\hat{\mathsf{A}}\rangle * \mathsf{F}(s), \tag{2.6}$$

where $\beta \equiv 1/k_B T$, $\langle \cdots \rangle_{NE}$ and $\langle \cdots \rangle$ denote nonequilibrium and equilibrium grand canonical averages, respectively, $\dot{B}(t)$ is the time derivative of the mechanical operator B, and the subscript $Kubo$ indicates a so-called Kubo transform, namely,

$$B_{Kubo}(t) \equiv \int_0^1 d\lambda \, B(t - i\beta\hbar\lambda), \tag{2.7}$$

and, of course, is necessary only for quantum systems.

In a relaxation experiment, the system is removed from equilibrium by adiabatically switching on the external fields; when $t=0$ is reached, the fields are removed, and the system relaxes back to equilibrium. Under these circumstances, Eq. (2.6) gives

$$\hat{b}(t) = \begin{cases} \langle \hat{B}_{Kubo}(0)\hat{\mathsf{A}} \rangle * \beta \mathsf{F} & \text{for } t \leqslant 0, \\ \langle \hat{B}_{Kubo}(t)\hat{\mathsf{A}} \rangle * \beta \mathsf{F} & \text{for } t > 0, \end{cases} \tag{2.8}$$

where we have assumed $\mathsf{F}(t) = e^{\epsilon t}\mathsf{F}$ for $t \leqslant 0$, $\epsilon \to 0+$.

Equation (2.8) is not quite what we want; it gives the average deviation from equilibrium in terms of the initial values of the external fields used to produce the nonequilibrium state, and as such, long-range effects, like those associated with the boundaries of the system, may have to be considered when calculating the time correlation functions. Moreover, we will require the correlation functions for macroscopic times. Both of these difficulties are associated with the macroscopic behavior of the system, behavior well described by phenomenological equations, like the hydrodynamic equations, etc. On the other hand, we expect that many quantities have simple constitutive laws giving them in terms of some finite set of nonequilibrium state variables that specify the long-time and -length scale phenomena; e.g., the densities of conserved quantities or broken-symmetry variables.

To obtain this constitutive relation, at least in the linear approximation, we simply use Eq. (2.8) to express $\beta\mathsf{F}$ in terms of the deviations of the state variables (the $\hat{a}$'s) and then use the result for an arbitrary average; for a classical system, this gives

$$\hat{b}(t) = \langle \hat{B}(t)\hat{\mathsf{A}} \rangle * \langle \hat{\mathsf{A}}(t)\hat{\mathsf{A}} \rangle^{-1} * \hat{\mathsf{a}}(t) \tag{2.9a}$$

$$= \left[\langle \hat{B}\hat{\mathsf{A}} \rangle * \langle \hat{\mathsf{A}}\hat{\mathsf{A}} \rangle^{-1} - \int_0^t ds \langle \dot{B}^{\ddagger}(s)\dot{\mathsf{A}}^{\ddagger} \rangle * \langle \hat{\mathsf{A}}(s)\hat{\mathsf{A}} \rangle^{-1} \right] * \hat{\mathsf{a}}(t), \tag{2.9b}$$

where, henceforth, we focus on classical systems, and drop the *Kubo* subscripts. The quantity

$$\dot{B}^{\ddagger}(s) \equiv \dot{B}(s) - \langle \dot{B}(s)\hat{\mathsf{A}} \rangle * \langle \hat{\mathsf{A}}(s)\hat{\mathsf{A}} \rangle^{-1} * \hat{\mathsf{A}}(s) \tag{2.10}$$

is called the dissipative part of $\dot{B}(s)$, and is the part of the rate of change of B *not* described by the linearized macroscopic equations [cf. Eq. (2.9b)]. In particular, when the time scales associated with the A's are much longer than that of B, as can be the case for the densities of conserved variables in the zero-wave-vector limit, one can evaluate the time correlation functions containing the A's at zero time.

Equation (2.9b) generalizes the well known Green-Kubo relations for the transport coefficients [which are obtained if Eq. (2.9b) is used for the stress tensor or energy current]. There are alternate derivations of this result and the derivation can be extended to nonlinear order or further resummed in several ways (see Ref. [9]).

Here we are interested in the nonequilibrium singlet generic distribution function in a system subjected to a uniform shear. This corresponds to taking

$$B(\boldsymbol{r},\boldsymbol{p};t) \equiv \sum_{i=1}^{N} \delta(\boldsymbol{r} - \boldsymbol{r}_i(t))\delta(\boldsymbol{p} - \boldsymbol{p}_i(t)), \tag{2.11}$$

where $\boldsymbol{r}_i$ and $\boldsymbol{p}_i$ are the position and momentum of the ith particle, respectively. By taking the nonequilibrium state variables A to be the densities of the conserved variables, energy (E), number (N), and momentum ($\boldsymbol{P}$), and by assuming a steady uniform shear gradient Eq. (2.9b) becomes

$$\phi_{NE}(\boldsymbol{r},\boldsymbol{p};t) \equiv \rho^{-1}\langle B(\boldsymbol{r},\boldsymbol{p};t) \rangle_{NE} = \phi(\boldsymbol{p})[1 + \beta \boldsymbol{p} \cdot \boldsymbol{v}(\boldsymbol{r})] + \Delta\overleftrightarrow{\Phi}(\boldsymbol{p}) : \nabla \boldsymbol{v}(\boldsymbol{r}), \tag{2.12}$$

where $\rho \equiv N/V$ is the number density, $\boldsymbol{v}(\boldsymbol{r}) \equiv \boldsymbol{p}(\boldsymbol{r})/m\rho(\boldsymbol{r})$ is the local velocity,

$$\phi(p) \equiv \frac{e^{-p^2/2mk_BT}}{(2\pi m k_B T)^{3/2}} \tag{2.13}$$

is the equilibrium momentum distribution, m is the mass of the particles,

$$\Delta\overleftrightarrow{\Phi}(\boldsymbol{p}) \equiv \int_0^{\infty} dt \frac{\left\langle \sum_i \delta(\boldsymbol{p} - \boldsymbol{p}_i(t)) \overleftrightarrow{\tau}_T^{\ddagger} \right\rangle}{N k_B T}, \tag{2.14}$$

$$\overleftrightarrow{\tau}_T \equiv \sum_i \frac{\boldsymbol{p}_i \boldsymbol{p}_i}{m} + \frac{1}{2} \sum_{j \neq i} \boldsymbol{r}_{i,j} \boldsymbol{F}_{i,j} \tag{2.15}$$

is the well known expression for the stress tensor in a one-component system interacting through pairwise additive forces, and [see Eq. (2.10)]

$$\overleftrightarrow{\tau}_T^{\ddagger} = \hat{\overleftrightarrow{\tau}}_T - \overleftrightarrow{\mathbb{I}} \left[\left(\frac{\partial p_h}{\partial \rho} \right)_e \hat{N} + \left(\frac{\partial p_h}{\partial e} \right)_{\rho} \hat{E} \right], \tag{2.16}$$

where p_h is the equilibrium pressure and $e \equiv \langle E \rangle / V$. In obtaining Eqs. (2.12) and (2.16) some simple equilibrium momentum averages have been carried out.

The first of the nonequilibrium terms in Eq. (2.12) has a trivial origin; namely, it is there to correct the equilibrium distribution to the local rest frame, or local equilibrium, of the fluid (here to linear order) and is analogous to what is found in the leading order Chapman-Enskog solution of the Boltzmann equation (cf. Ref. [1]). By using the methods of Ref. [9], it is straightforward to show that this is no accident, and that all the higher-order nonlinear corrections arising

from the transformation to a local rest frame are present and can be resummed to show that

$$\phi(\boldsymbol{p}) \to \phi(\boldsymbol{p} - m\boldsymbol{v}(\boldsymbol{r})). \tag{2.17}$$

In general, this is a trivial effect, and henceforth we assume that the measurement is done in the local rest frame, i.e., $\boldsymbol{v}(\boldsymbol{r}) = \boldsymbol{0}$.

On the other hand, the last of the nonequilibrium terms in Eq. (2.12) does not have a trivial origin, and its computation is the main objective of this work. The time correlation function in Eq. (2.14) is also a tensor function of the momentum, and as such will be more difficult to simulate than the Green-Kubo time correlation functions for the standard transport coefficients.

Some simplification can be obtained by considering steady states or incompressible fluids, and we assume this henceforth. In either case, $\boldsymbol{\nabla} \cdot \boldsymbol{v}(\boldsymbol{r}) = 0$, and thus, the diagonal parts of the time correlation function may be omitted.

Symmetry can be used to further simplify the expression; in an isotropic system, it follows that the integrand appearing in Eq. (2.14) can be written as

$$\overleftrightarrow{C}(\boldsymbol{p},t) \equiv \frac{\left\langle \sum_i \delta(\boldsymbol{p} - \boldsymbol{p}_i(t)) \overset{\circ}{\overleftrightarrow{\tau}}_T \right\rangle}{N k_B T} = \left(\hat{\boldsymbol{p}}\hat{\boldsymbol{p}} - \frac{1}{3}\overleftrightarrow{\mathbb{I}} \right) C(p,t), \tag{2.18}$$

where the $\circ$ denotes the traceless part, and where

$$C(p,t) = \frac{3\left\langle \sum_i \delta(p - p_i(t)) \boldsymbol{p}_i(t)\boldsymbol{p}_i(t) : \overset{\circ}{\overleftrightarrow{\tau}}_T \right\rangle}{8N\pi k_B T p^4}. \tag{2.19}$$

This last result is obtained by doubly contracting with momentum vectors and integrating over a unit momentum sphere. Note that the δ function is for the *magnitude* of the momentum, and gives some sampling advantages in the numerical work to be presented below.

B. Sonine polynomial expansion

Another way in which to simplify the calculation of the correlation functions needed for the distribution function is to consider an expansion in terms of some convenient complete set of functions, thereby avoiding the sampling issues associated with the δ functions that appear in Eq. (2.19). In Ref. [6] it was shown how the general expressions for $\Delta\overleftrightarrow{\Phi}(\boldsymbol{p})$ give results identical to those of the Chapman-Enskog solution to the Boltzmann equation to leading order in density. Hence, this suggests that we use the same functions as those used in the Chapman-Enskog theory, and as a by-product this choice will allow us to easily study the range of validity of the low-density results.

The Chapman-Enskog solution gives an integral equation for the correction to the distribution function that is solved by expanding in Sonine polynomials. Thus we write

$$\Delta\overleftrightarrow{\Phi}(\boldsymbol{p}) = 2\left(\boldsymbol{\zeta}\boldsymbol{\zeta} - \frac{1}{3}\zeta^2 \overleftrightarrow{\mathbb{I}} \right) \sum_{n=0}^{\infty} b_n L_n^{5/2}(\zeta^2)\phi(p), \tag{2.20}$$

where $L_n^{5/2}(x)$ is a generalized Laguerre polynomial (or Sonine polynomial) [1], $\boldsymbol{\zeta} \equiv \boldsymbol{p}/\sqrt{2mk_BT}$ is a reduced momentum, and the factor of 2 was introduced to follow Chapman and Cowling's notation. By using the orthogonality properties of the Sonine polynomials (see Ref. [1] or [10]), it is straightforward to show that

$$b_n = \frac{n!\Gamma(\frac{7}{2})}{10mk_BT\Gamma(\frac{7}{2}+n)} \int d\boldsymbol{p}\, L_n^{5/2}(\zeta^2)\boldsymbol{p}\boldsymbol{p} : \Delta\overleftrightarrow{\Phi}(\boldsymbol{p}). \tag{2.21}$$

Lastly, by using the linear response expression for $\Delta\overleftrightarrow{\Phi}(\boldsymbol{p})$ [cf. Eq. (2.14)] it follows that

$$b_n = \frac{n!\Gamma(\frac{7}{2})}{10\Gamma(\frac{7}{2}+n)} \int_0^{\infty} dt \frac{\left\langle \sum_i L_n^{5/2}(\zeta_i^2(t))\boldsymbol{p}_i(t)\boldsymbol{p}_i(t) : \overset{\circ}{\overleftrightarrow{\tau}}_T \right\rangle}{m(k_bT)^2 N}. \tag{2.22}$$

These coefficients will be evaluated in the molecular dynamics work to be presented below.

C. Molecular dynamics

The time correlation functions were calculated in a conventional molecular dynamics (MD) simulation. Following Verlet (see Ref. [11]), a system of 864 particles were placed on a face-centered cubic lattice and the dimensions of the cell adjusted so as to give the desired density of the gas or liquid. An initial set of velocities is assigned, drawn from a Maxwell-Boltzmann distribution appropriate to the temperature of interest, with a total linear momentum equal to zero. The temperature was reequilibrated during aging by calculating the average kinetic energy and rescaling the velocities to give the desired kinetic temperature; this was repeated until the average was within 0.25% of the desired value; thereafter, it was allowed to fluctuate, and a further aging period was performed before starting any averages.

Trajectories for all the particles were computed by integrating the equations of motion using the Schofield algorithm (see Ref. [12]), periodic boundary conditions, and Verlet's bookkeeping technique for handling the interactions [11]. The coordinates and momenta of the particles as well as the forces acting on every particle were stored, and thermodynamic and other properties were calculated as discrete time averages over the dynamical history of the system.

The bining over momenta involved in computing $C(p,t)$ [cf. Eq. (2.19)], increases the sampling error in the simulation, especially for improbable momenta (i.e., for $p \to 0$ or $p \to \infty$), and consequently very long averages must be performed. It is neither practical nor necessary to store the entire dynamical history of the quantities of interest in order to

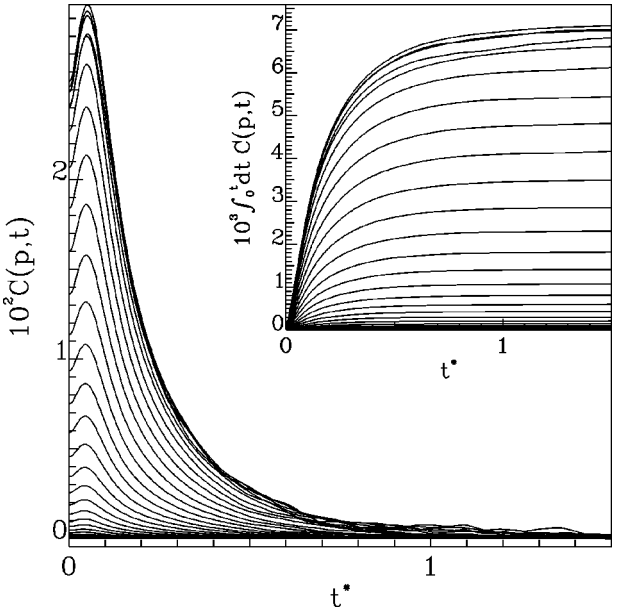

FIG. 1. The correlation function $C(p,t)$ (in the reduced units described at the beginning of Sec. III) for $T^*=1.5$ and $\rho^*=0.5$ for reduced momenta equally spaced in the range $1.5\leqslant p^*\leqslant 7.5$. The averages were obtained by averaging the results of 16 independent runs, each of length 10^4 (in reduced units).

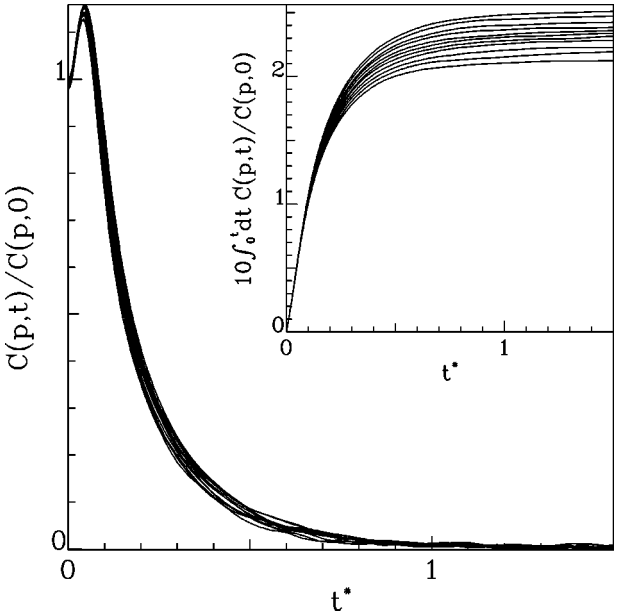

FIG. 2. The reduced correlation function $C(p,t)/C(p,0)$ for the 11 largest $C(p,t)$'s shown in Fig. 1. The inset shows the time integrals decreasing in order of increasing momentum (cf. Fig. 3 below).

compute their correlation functions. Since the calculation of the time correlation functions will involve expressions of the form

$$C(t)=\frac{1}{M}\sum_{s=0}^{M-1}A(t+s)B(s), \tag{2.23}$$

where typically $0\leqslant t\leqslant T_{max}\ll M$ (integer times are assumed here), the convolution can easily be performed using fast Fourier transforms (FFT's) and a variant of the overlap-add method [13]. The sum is decomposed into N_B blocks of M' terms and Eq. (2.23) is rewritten as

$$C(t)=\frac{1}{N_BM'}\sum_{m=0}^{N_B-1}\sum_{s=0}^{M'-1}A(t+s+mM')B(s+mM'). \tag{2.24}$$

The innermost convolution is early performed by zero-padding B and then using a FFT for $M+T_{max}$ points. The results for the different m-blocks are then added together [in practice, this requires one to save the values for $A(t)$ and $B(t)$ for $(m+1)M'\leqslant t\leqslant(m+1)M'+T_{max}$ before zero padding].

III. RESULTS AND DISCUSSION

The theory described in the preceding section was implemented for particles interacting through Lennard-Jones 6-12 potentials

$$u(r)\equiv 4\epsilon\left[\left(\frac{\sigma}{r}\right)^{12}-\left(\frac{\sigma}{r}\right)^{6}\right]. \tag{3.1}$$

In the numerical work, units where $\sigma=1$, $m=1$, and $\epsilon=1$ are used; and we define the reduced temperature, density, time, and momentum as $T^*\equiv k_BT/\epsilon$, $\rho^*\equiv\rho\sigma^3$, $t^*\equiv t\sqrt{\epsilon/m\sigma^2}$, and $p^*\equiv p/\sqrt{m\epsilon}$, respectively. Note that the reduced time differs from Verlet's [11], by a factor of $\sqrt{48}$. Like Verlet [11], we use a potential cutoff at a distance of 2.5σ, a maximum radius for the bookkeeping table (which is updated every 16 time steps) of 3.3σ, a reduced time step of 4.6188×10^{-3}, and an aging time of 1.4434. For argon, $\epsilon/k_B=116$ K and $\sigma=3.465$ Å [14], thus resulting in a time step and an aging time of 1.03×10^{-14} and 3.2×10^{-12} s, respectively. A typical average was about 10^{-8}–10^{-7} s long.

Figure 1 shows the time correlation function correlation $C(p,t)$ as a function of time for a reduced density of 0.5 and reduced temperature of 1.5. The inset shows the time integral $\int_0^t dt\ C(p,t)$ and shows that the integrals plateau on a microscopic time scale. The different curves are for uniformly chosen values of reduced momentum p^*. In general, the overall magnitude of $C(p,t)$ follows $C(p,0)\propto p^2\phi(p)$ [cf. Eq. (A1)]. The relative noise increases as the tails of the distribution or long times are approached, the latter as expected from the analysis in Ref. [15].

Note the initial rise of all the correlation functions; as is shown in the Appendix, the initial curvature is, in general, positive for the 6-12 potential, and our data are consistent with this analysis [cf. Eq. (A8)]. The short-time analysis also predicts that the initial curvature in the reduced correlation function $C(p,t)/C(p,0)$ should be independent of momentum. This short-time behavior is confirmed in Fig. 2, although the behavior at longer times (and consequently in the integral) depends on the momentum.

A momentum-dependent relaxation time is defined as

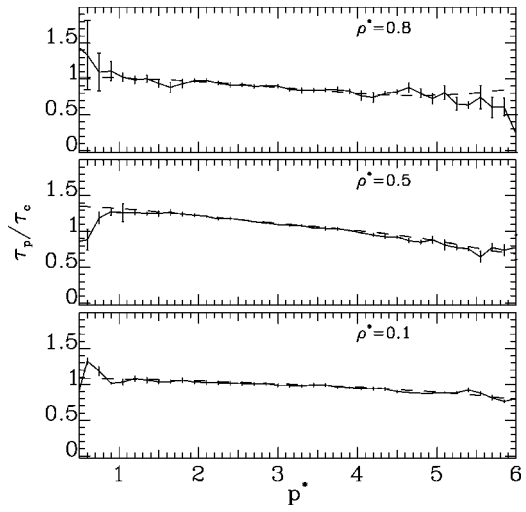

FIG. 3. The ratio of the momentum-dependent relaxation time to the collision time, $\tau_c = 1/[4(\pi k_B T/m)^{1/2}\rho\sigma^2]$, for $T^* = 1.5$ for the reduced densities shown. The dashed curves are obtained from a five-term Sonine polynomial expansion. The error bars represent two standard deviations. Note that the nonequilibrium correction will be largest roughly at $p^* \sim \sqrt{2T^*}$.

$$\tau_p \equiv \int_0^\infty dt \frac{C(p,t)}{C(p,0)}, \tag{3.2}$$

and is shown in Fig. 3. The error is largest at either small or large momenta, since the probability of observing these momenta is small and the statistics are poorest; this leads to the large statistical errors indicated in Fig. 3.

It is interesting to note that the relaxation time is roughly linear in momentum in the portion of the figure where the statistical error is small. Moreover, the variation is not very large. Figure 3 also shows the result of summing the Sonine polynomial expansion [cf. Eq. (2.20)], using the coefficients computed from Eq. (2.22) as reported in Table I. In both methods, integrals of the required time correlation functions were numerically computed between 0 and t, and the long-time results fitted to a constant. Note that the error will increase as the order of the Sonine expansion coefficient is increased, since these have increased weight from higher momenta, where the statistical error is greater.

Table II gives the prediction of the Boltzmann equation, obtained from a three term expansion using the method described in Ref. [1] and using the collision integrals tabulated in Ref. [2]. As was mentioned above, the theory is supposed to give results equivalent to that of the Chapman-Enskog expansion as $\rho \to 0$. By comparing the lowest-density data in Tables I and II we see that this is indeed the case; the nonequilibrium correction is dominated by the leading term and the agreement is excellent (about 1% in the leading coefficient), especially given that there are truncation errors associated with the method used to calculate the low-density results. In addition, remember that we are using a cutoff potential in the simulations, and that significant corrections (e.g., in the pressure) must be introduced in some quantities in order to get accurate results for the full-range potentials. Unlike a static quantity like the pressure, it is not clear what this correction should be and none was introduced here. It seems that they are not too important for $C(p,t)$; the reason for this may be that only the traceless part of the stress is involved, and the underlying correlations may be shorter ranged.

The second order Chapman-Enskog correction to the distribution function is inversely proportional to the density, and thus the Sonine polynomial expansion coefficients in the Boltzmann equation are as well. This is clearly *not* the case for the data shown in Table I. On the other hand, there is at least one important point of similarity between the higher-density results and the prediction of the Boltzmann equation; namely, for the more probable momenta, i.e., $p \sim \sqrt{2mk_BT}$, the nonequilibrium correction to the distribution function is dominated by the contribution from the zeroth order Sonine polynomial. Hence, a simple, albeit *ad hoc*, correction to the Boltzmann equation would be to multiply the collision term by some density- and temperature-dependent factor. In practice, this is precisely what happens with the Enskog modification to the Boltzmann equation in steady shear flow (cf. Ref. [1], Sec. 16.33) for dense hard sphere gases. Moreover, in the Enskog approximation it turns out that

$$\Delta\vec{\Phi}(\boldsymbol{p}) \to \frac{1+\frac{2}{5}b\rho\chi}{\chi}\Delta\vec{\Phi}_B(\boldsymbol{p}), \tag{3.3}$$

where $b \equiv \frac{2}{3}\pi\sigma^3$ and $\Delta\vec{\Phi}_B(\boldsymbol{p})$ is the second order Chapman-Enskog correction to the distribution function obtained from the Boltzmann equation, e.g., as can be constructed using the Sonine polynomial expansion coefficients given in Table II. In addition, χ and the equilibrium pressure p_h are related as

$$p_h = \rho k_B T(1 + b\rho\chi), \tag{3.4}$$

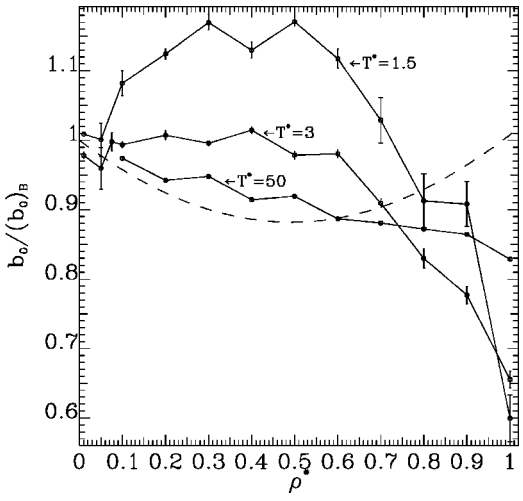

FIG. 4. The ratio of the leading Sonine polynomial expansion coefficient to the value predicted by the Boltzmann equation (see Table II) for the indicated reduced temperatures. The dashed line is the prediction of the Enskog theory for hard spheres, using a seven-term virial expansion for the pressure. The error bars represent one standard deviation.

TABLE I. Sonine polynomial expansion coefficients. The reported uncertainty is one standard deviation.

ρ^*	b_0	b_1	b_2	b_3	b_4
			$T^*=1.5$		
0.01	11.059±0.004	0.10±0.02	−0.05±0.02	0.069±0.007	−0.066±0.005
0.1	1.19±0.02	0.020±0.004	0.006±0.002	0.0±0.001	0.002±0.001
0.2	0.616±0.004	0.008±0.002	0.007±0.005	0.001±0.001	−0.003±0.001
0.3	0.427±0.004	0.0081±0.0005	0.0016±0.0004	0.0006±0.0002	0.0022±0.0005
0.4	0.310±0.003	0.011±0.001	0.004±0.001	−0.0007±0.0005	−0.0008±0.0004
0.5	0.257±0.001	0.011±0.001	0.0033±0.0006	0.0011±0.0005	0.0007±0.0003
0.6	0.204±0.003	0.008±0.002	0.0025±0.0005	0.0008±0.0004	−0.0003±0.0002
0.7	0.161±0.005	0.010±0.002	0.0±0.0007	0.0001±0.0009	−0.0004±0.0005
0.8	0.125±0.005	0.0±0.002	0.0015±0.0008	0.0007±0.0005	0.001±0.001
0.9	0.111±0.004	0.0±0.002	0.0012±0.0009	−0.0013±0.0007	0.0±0.0009
1.0	0.066±0.004	0.001±0.001	−0.002±0.002	0.002±0.001	0.0±0.0005
			$T^*=3.0$		
0.01	9.62±0.05	0.27±0.03	−0.014±0.006	−0.018±0.009	−0.0363±0.005
0.1	0.977±0.004	0.039±0.001	0.0010±0.0008	0.0±0.007	0.0±0.001
0.2	0.495±0.003	0.0178±0.0005	0.0021±0.0005	0.0026±0.0005	0.0010±0.0002
0.3	0.326±0.001	0.0130±0.0006	−0.0007±0.0004	0.0±0.0002	0.0003±0.0002
0.4	0.249±0.001	0.0125±0.0003	0.0022±0.0003	0.0014±0.0001	0.0±0.0001
0.5	0.192±0.001	0.0102±0.0006	0.0019±0.0002	0.0002±0.0002	0.00003±0.00007
0.6	0.1606±0.0009	0.005±0.001	0.0006±0.0002	−0.0014±0.0002	−0.0012±0.0005
0.7	0.1277±0.0009	0.0063±0.0004	−0.0003±0.0003	−0.0001±0.0002	0.0±0.0001
0.8	0.102±0.002	0.0063±0.0008	0.0012±0.0002	0.0006±0.0002	0.00006±0.00009
0.9	0.085±0.001	0.0006±0.0004	0.0005±0.0002	0.0005±0.0003	−0.0004±0.0002
1.0	0.064±0.001	0.0014±0.0004	0.0±0.0004	0.0002±0.0002	0.0003±0.0002
			$T^*=50.0$		
0.1	0.3764±0.0006	0.0176±0.0005	0.0021±0.0002	0.0020±0.0005	0.0±0.0002

and hence χ can easily be expressed in terms of the coefficients in the virial expansion of the pressure or in terms of the hard-sphere pair cavity function at contact.

The ratio of b_0 to its Boltzmann equation value is shown in Fig. 4 along with the Enskog prediction. Although the differences between this work and the Enskog prediction decrease as the temperature is increased, clearly, very different trends are observed. One possible explanation for this lies in what the Enskog modification includes; for shear flow, this is primarily the effect of a higher average local density, and hence a higher collision rate at the collision radius. In terms of this work, a higher collision rate should lead to a faster decay of correlations, and indeed this is seen when looking at the decay's of $C(p,t)$ for different densities; i.e., they decay faster than would be expected simply based on the collision rate τ_c^{-1}. This alone would lead to a reduction of τ_p compared with the prediction of the Boltzmann equation. However, neither the Enskogn or the Boltzmann equation explicitly includes the elastic effects discussed in the Appendix, and as we have shown, these lead to an enhancement of $C(p,t)$. This apparently overcomes the shorter decay time at intermediate densities, thereby resulting in a net increase in τ_p/τ_c (see Fig. 4). Indeed, the extent of the initial rise decreases as the temperature is increased, and closer agreement with the Enskog prediction is obtained.

Of course, there are deviations from what is predicted by the Boltzmann and Boltzmann-Enskog equations, even with a fitted collision rate. For example, we find that b_1/b_0 varies with density (see Table I), while the Boltzmann-Enskog ratio remains constant (e.g., at $T^*=1.5$, $\rho^*=0.5$, $b_1/b_0=0.043$ compared with the Boltzmann-Enskog prediction of 0.01; see Table II). This is also clearly seen in the variation of τ_p/τ_c with momentum shown in Fig. 3.

TABLE II. Chapman-Enskog Sonine polynomial expansion coefficients.

T^*	$\rho^* b_0$	$\rho^* b_1$	$\rho^* b_2$
1.5	0.109599	0.00100065	−0.000204088
3.0	0.098303	0.00279743	0.000145408
50.0	0.0386414	0.00168169	0.000234626

IV. CONCLUDING REMARKS

In this work we have shown how to apply response theory and computer simulation to the calculation of the nonequilibrium velocity distribution function in the linear regime, and at arbitrary densities. As expected, results equivalent to those obtained from the Boltzmann equation are obtained in the limit of infinite dilution, but qualitative deviations from the prediction of the Boltzmann or Boltzmann-Enskog equa-

tion set in as the density is increased. Surprisingly, the functional form of the first correction to the Boltzmann equation reasonably describes what is obtained from response theory; however, the amplitude deviates from what is predicted by either the Boltzmann or the Boltzmann-Enskog equation. As was argued in the preceding section, this is likely due to the short-time elastic effects not present in the low-density theories. That the Enskog theory makes reasonable predictions for kinetic contributions to the hard-sphere transport coefficients has been known for some time [16]; however, as we have shown here, the underlying reason for this is much more general, namely, the full single particle velocity distribution is dominated by the first Sonine polynomial and thus has the same functional form as those predicted by the Boltzmann-Enskog equations.

ACKNOWLEDGMENT

A portion of this work was supported by the National Science and Engineering Research Council of Canada.

APPENDIX: SHORT-TIME EXPANSION

Here we consider the short-time expansion of the time correlation function $C^{\alpha,\beta}(\boldsymbol{p},t)$ [Eq. (2.18)]. It is straightforward to obtain the first few terms in the Taylor expansion. At $t=0$ it is easy to show that

$$C(p,0)=\frac{p^2\phi(p)}{mk_BT}, \tag{A1}$$

where $\phi(p)$ is the equilibrium momentum distribution function [see Eq. (2.13)].

The next order terms are slightly more complicated. First, note that for isotropic systems $C^{\alpha,\beta}(\boldsymbol{p},t)$ is an even function of $\boldsymbol{p}$. This, combined with time-reversal symmetry, implies that it is also an even function of t, and hence the next nonvanishing term requires the second order time derivative. It is easy to show that

$$\ddot{C}^{\alpha,\beta}(\boldsymbol{p},0)=\frac{\partial}{\partial p^\gamma}\frac{\langle\delta(\boldsymbol{p}-\boldsymbol{p}_i)F_i^\gamma\dot{\tau}^{\alpha,\beta}\rangle}{Nk_BT}, \tag{A2}$$

where

$$\dot{\tau}^{\alpha,\beta}=\frac{2p_i^\alpha F_i^\beta+p_i^\beta F_i^\alpha}{m}+r_i^\alpha\frac{\partial F_i^\beta}{\partial r_j^\gamma}\frac{p_j^\gamma}{m}, \tag{A3}$$

and where, henceforth, repeated indices are summed. In obtaining Eq. (A2) one of the time derivatives was moved to the stress tensor and the overall sign changed (the so-called dot-switching property), by using the fact that the equilibrium average is stationary. The various momentum averages are easily done and Eq. (A2) becomes

$$\begin{aligned}\ddot{C}^{\alpha,\beta}(\boldsymbol{p},0)&=\frac{\partial}{\partial p^\gamma}\left[\frac{\phi(p)}{mNk_BT}\left(2p^\alpha\langle F_i^\gamma F_i^\beta\rangle\right.\right.\\&\quad\left.\left.+p^\beta\langle F_i^\gamma F_i^\alpha\rangle+p^\sigma\left\langle r_i^\alpha\frac{\partial F_i^\beta}{\partial r_j^\sigma}F_j^\gamma\right\rangle\right)\right]\\&=-\frac{\phi(p)}{N(mk_BT)^2}\left(p^\alpha p^\beta\langle F_i^\gamma F_i^\gamma\rangle\right.\\&\quad\left.+p^\gamma p^\sigma\left\langle r_i^\alpha\frac{\partial F_i^\beta}{\partial r_j^\sigma}F_j^\gamma\right\rangle\right),\end{aligned} \tag{A4}$$

where the second equality is obtained by dropping terms that are diagonal in α,β. The final step involves replacing the last force factors by momentum time derivatives, again using the dot-switching property, and performing the resulting momentum integrations; this gives

$$\begin{aligned}\ddot{C}^{\alpha,\beta}(\boldsymbol{p},0)&=\frac{\phi(p)}{m^2Nk_BT}\left(\frac{4}{3}\langle\boldsymbol{\nabla}_i\cdot\boldsymbol{F}_i\rangle p^\alpha p^\beta\right.\\&\quad\left.+\left\langle r_i^\alpha\frac{\partial^2F_i^\beta}{\partial r_j^\sigma\partial r_j^\gamma}\right\rangle p^\sigma p^\gamma\right)\\&=-\frac{8\pi\rho\phi(p)p^\alpha p^\beta}{15m^2k_BT}\int_0^\infty dr\,g^{(2)}(r)r[r^2u'''(r)\\&\quad+12ru''(r)+18u'(r)],\end{aligned} \tag{A5}$$

where the second equality is obtained for isotropic systems interacting through a pairwise additive pair potential $u(r)$, $g^{(2)}(r)$ is the pair correlation function, and diagonal terms have again been dropped.

It is easy to show that the right hand side of Eq. (A5) is negative for any repulsive power-law potential $u(r)\equiv\epsilon(\sigma/r)^\alpha$, with $1<\alpha<8$, and is positive otherwise. In fact, for such potentials

$$\ddot{C}^{\alpha,\beta}(\boldsymbol{p},0)=\frac{8\pi\rho\phi(p)p^\alpha p^\beta\sigma(\beta\epsilon)^{1/\alpha}(\alpha-1)(\alpha-8)}{15m^2}\int_0^\infty dz\,z^{-1/\alpha}e^{-z}y^{(2)}(\sigma[z/(\beta\epsilon)]^{-1/\alpha}) \tag{A6a}$$

$$\sim\frac{8\pi\rho\phi(p)p^\alpha p^\beta\sigma(\beta\epsilon)^{1/\alpha}y^{(2)}(\sigma)\alpha^2(1-8/\alpha)\Gamma(2-1/\alpha)}{15m^2}\ \text{as}\ \alpha\to\infty\ \ \text{or}\ \ \rho\to0, \tag{A6b}$$

where $y^{(2)}(r)$ is the pair cavity function. Note that the initial curvature diverges as the hard-sphere limit is approached (i.e., $\alpha\rightarrow\infty$) and probably signals nonanalytic short-time dependence (e.g., as $|t|$). For the 6-12 potential and units used in this work, Eq. (A5) gives

$$\ddot{C}^{\alpha,\beta}(\boldsymbol{p},0)=\frac{128\pi\rho\phi(p)p^{\alpha}p^{\beta}}{5T}\int_0^{\infty}dr\,g^{(2)}(r)\frac{5r^6+44}{r^{12}}, \tag{A7}$$

which explains why the observed initial curvature is always positive.

By combining Eqs. (A1) and (A5), we see that

$$C(p,t)\sim\frac{p^2\phi(p)}{mk_BT}\left(1-t^2\frac{4\pi\rho}{15m}\int_0^{\infty}dr\,g^{(2)}(r)r[r^2u'''(r)+12ru''(r)+18u'(r)]\right). \tag{A8}$$

Thus, the initial relative curvature, i.e., in $C(p,t)/C(p,0)$, is the same for all momenta. Its origin is elastic in nature and involves averages similar to those found in the classic work of Zwanzig and Mountain [17].

[1] S. Chapman and T.G. Cowling, *The Mathematical Theory of Non-Uniform Gases* (Cambridge University Press, Cambridge, England, 1970).

[2] J.O. Hirshfelder, C.F. Curtiss, and R.B. Bird, *Molecular Theory of Gases and Liquids*, 2nd ed. (Wiley, New York, 1964), Chaps. 7 and 8. In particular, the collision integrals reported in Table I-M on p. 1126 were used.

[3] P. Resibois and M. De Leener, *Classical Kinetic Theory of Fluids* (Wiley, New York, 1977).

[4] For a review, see, e.g., A.-M.S. Tremblay, in *Recent Developments in Nonequilibrium Thermodynamics*, edited by J. Casas-Vasquez, D. Jou, and G. Lebon (Springer-Verlag, Berlin, 1984), pp. 267–315.

[5] I. Procaccia, D. Ronis, M.A. Collins, J. Ross, and I. Oppenheim, Phys. Rev. A **19**, 1290 (1979).

[6] D. Ronis, I. Procaccia, and I. Oppenheim, Phys. Rev. A **19**, 1307 (1979).

[7] D. Ronis, I. Procaccia, and I. Oppenheim, Phys. Rev. A **19**, 1324 (1979).

[8] R. Kubo, J. Phys. Soc. Jpn. **12**, 570 (1957).

[9] D. Ronis, Physica A **99**, 403 (1979).

[10] *Handbook of Mathematical Functions*, edited by M. Abramowitz and I. Stegun, Natl. Bur. Stand. Appl. Math. Ser. No. 55 (U.S. GPO, Washington, DC, 1970), Chap. 22.

[11] L. Verlet, Phys. Rev. **159**, 98 (1967); also see, G. Ciccotti, D. Frenkel, and I.R. McDonald, *Simulation of Liquids and Solids* (North-Holland, Amsterdam, 1987).

[12] P. Schofield, Comput. Phys. Commun. **5**, 17 (1973).

[13] See, e.g., W.H. Press, S.A. Teukolsky, W.T. Vetterling, and B.P. Flannery, *Numerical Recipes in C*, 2nd ed. (Cambridge University Press, Cambridge, England, 1994), Sec. 13.2.

[14] J.O. Hirshfelder, C.F. Curtiss, and R.B. Bird, *Molecular Theory of Gases and Liquids* (Ref. [2]), p. 1110, Table I-A.

[15] R. Zwanzig and N.K. Ailawadi, Phys. Rev. **182**, 280 (1969).

[16] B.J. Alder, D.M. Gass, and T.E. Wainwright, J. Chem. Phys. **53**, 3813 (1970).

[17] R. Zwanzig and R.D. Mountain, J. Chem. Phys. **12**, 4464 (1965).